

# The Effect of Temperature on the Electrochemistry of Titanium Dioxide Nano Material for Lithium Ion Batteries

NG Zheng Jie, Glenn<sup>1</sup>, PEH Long Quan<sup>1</sup>, M.V. Reddy<sup>2,3</sup>, S. Adams<sup>3</sup>, B.V.R. Chowdari<sup>2</sup>

<sup>1</sup> SRP students, Victoria Junior College

<sup>2</sup>Department of Physics, National University of Singapore, Singapore 117542

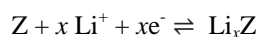
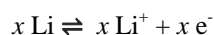
<sup>3</sup>Departments of Materials Science & Engineering, National University of Singapore, Singapore 117546

## I. Introduction

Lithium-ion batteries (LIBs) are integral to much of modern electronic devices today, due to the relatively low maintenance of the cell and the low level of self-discharging of the cell, maintaining a high energy capacity even with prolonged use. [Johnson, B., & White, R., 1998] Compared to other batteries such as lead-acid battery, the technology for lithium ion battery is relatively new, many aspects and much research can be done in this field.

LIBs consist of a separator, electrolyte, cathode of lithium metal and an anode of choice, usually a lithium compound denoted Z in this case.

Electrochemical mechanism:



During the charging process the lithium ions flow through the separator to form a compound with the anode,  $\text{Li}_x\text{Z}$ . The battery is now charged. During the discharging process, the Lithium ions flow back to the lithium metal layer and it is this flow of electrons that results in a current flow.

In spite of the advantages mentioned above, LIBs still have a variety of problems such as capacity fading (Arora, P. et. al, 1998), where the amount of charge delivered by the battery decreases with each charge-discharge cycle, and safety. (Doughty, D., & Roth, E., 2012)

Therefore, in order to further improve the working capacity of these cells, nanotechnology has been used to improve the materials used in the cell, which for the purposes of this research project will deal with the anode of the cell. Titanium dioxide ( $\text{TiO}_2$ ) is the proposed research material. Through prior research, it was found that the crystalline structure of titanium dioxide allows for a large surface area for electrochemical interactions with lithium ions in the cell, serving as an excellent low voltage insertion host for Li ions and a fast Li ion insertion/extraction host. [Khataee, A., & Mansoori, G., 2012] In addition, titanium dioxide nanotubes when fabricated into an electrode for LIBs, show a

maximum areal capacity of  $77 \mu\text{A h cm}^{-2}$ , a good capacity retention up to 90% over 50 cycles [Ortiz, G., et. al, 2009]. This evident interest in titanium dioxide as a material to be used for electrochemical processes has led us to believe that this material would be highly effective in improving cells. However, little research has been done on the different structures of  $\text{TiO}_2$ . It is known that  $\text{TiO}_2$  has two main crystal structures, the anatase structure and the rutile structure [Reddy, M., Kishore, M. et. al, 2006]. The diagrams below show the unit cell of (a) rutile  $\text{TiO}_2$  and (b) anatase  $\text{TiO}_2$  (Fig 1). The unit cell characteristics are listed in Table 1.

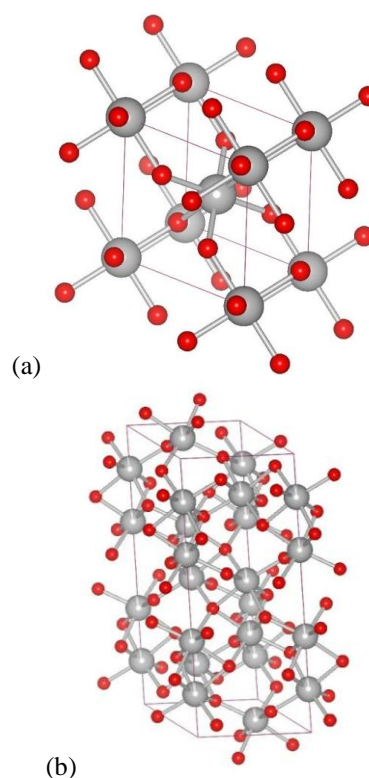


Figure 1: Unit cell structures of (a) rutile  $\text{TiO}_2$  and (b) anatase  $\text{TiO}_2$ , grey sphere is titanium and red is oxygen.

Table 1: Crystallographic properties of rutile and anatase [Khataee, A., & Mansoori, G., 2012]

Crystal Structure	System	Cell parameters (Å)	
		a	c
Anatase	Tetragonal	3.758	9.514
Rutile	Tetragonal	4.584	2.953

It is known that at higher temperatures, titanium dioxide would be in the anatase phase whereas at lower temperatures,  $\text{TiO}_2$  tends to be in the amorphous phase. [L. J. Alemany et al., 1999] At various temperatures, the crystal structure of titanium dioxide will change from one form to another, thereby affecting the final structure of  $\text{TiO}_2$  for use in LIBs. [L. J. Alemany et al., 1999] The different structures will alter the anode's capability to interact with lithium ions in the cell. Therefore the objective of this research is to investigate the effect of synthesis temperature.

The presence of the regular anatase structure at higher temperatures would cause the anode to possess a very high exposed surface area for ionic contact between the ions present in the  $\text{TiO}_2$  and the lithium ions present in the electrolyte. As such, we hypothesise that  $\text{TiO}_2$  synthesised at  $310^\circ\text{C}$  through the Molten Salt method would make the most effective anode, thus forming the cell with the highest performance in terms of capacity fading, and voltage vs current properties.

## II. Materials and Methods

### A. Synthesis of Titanium Dioxide

Various methods to synthesize titanium dioxide include the Sol-Gel method and Hydrothermal method. [Chen, X., & Mao, S., 2007] However, Molten Salt synthesis technique was used as titanium dioxide nanoparticles of high surface area over a range of temperatures can be prepared and is simple, offering an advantage. [Reddy et. al, 2015] Precursors consisting of titanium (IV) oxysulfate,  $\text{TiO}(\text{SO}_4)$ ; lithium nitrate,  $\text{LiNO}_3$ , sodium nitrate,  $\text{NaNO}_3$  and potassium nitrate,  $\text{KNO}_3$ , all purchased from Sigma-Aldrich, USA, were weighed and mixed in a ceramic crucible. The precursors were combined in a 1.00 mol  $\text{TiO}(\text{SO}_4)$ : 3.75 mol  $\text{LiNO}_3$ : 1.8 mol  $\text{NaNO}_3$ : 4.45 mol  $\text{KNO}_3$  mole ratio respectively and the total mass of the salts were scaled to 40.0 g. The crucible with the precursors was then placed into a furnace to heat

for a period of time. During the heating, the precursors melted and reacted, before crystallising into the final product once cooled. The temperature of the oven was varied, setting temperatures at  $310^\circ\text{C}$ ,  $180^\circ\text{C}$  and  $145^\circ\text{C}$ . These temperatures were chosen as they would result in different types of  $\text{TiO}_2$  structures. The electrochemical properties of the LIBs could then be investigated and any difference could be attributed to the structure of the  $\text{TiO}_2$ . The samples were all heated for 2 hours, with a heating/cooling rate of  $3^\circ\text{C}/\text{min}$ .

### B. Electrode Fabrication

To make the anodes, a slurry was made with the  $\text{TiO}_2$  prepared. This slurry was made by mixing the prepared  $\text{TiO}_2$ , Super-P carbon black powder and polyvinylidene fluoride (PVDF, Kynar 2801) in a 70:15:15 mass ratio. N-methyl-2-pyrrolidone (NMP) was added to disperse the solids in a suspension. The slurry was stirred into a uniform suspension for at least 12 hours. The anodic slurry was then poured onto an etched copper foil (acting as a substrate). Using a doctor blade, the slurry was spread evenly to form a uniform layer on the foil. The prepared anode was left to dry in an  $80^\circ\text{C}$  oven for 8 hours to evaporate the solvent. The copper foil was pressed using a stainless steel roller and the electrode was cut into circles of diameter 16 mm using a die. Next, the electrodes were weighed and placed in labelled battery caps (type CR2016) and left to dry in a vacuum oven at  $80^\circ\text{C}$  for at least 10 hours.

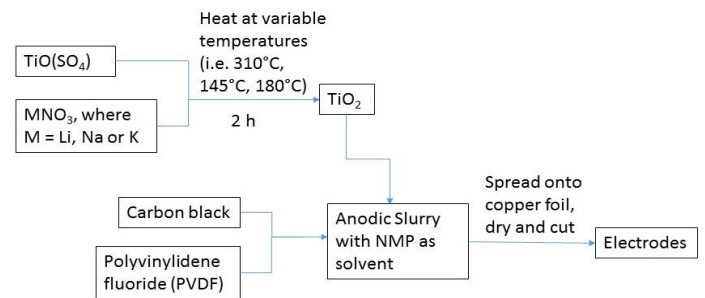


Figure 2: Overall synthesis process for making  $\text{TiO}_2$  electrodes

### C. Assembly of Lithium Ion Batteries

The electrodes and battery caps were brought inside an argon filled glove box to assemble the complete cell. Lithium metal serves as the cathode of the cell, while the  $\text{TiO}_2$  electrode serves as the anode. The electrodes were separated by a microporous separator soaked in a  $1\text{ mol dm}^{-3}$  solution of lithium hexafluorophosphate ( $\text{LiPF}_6$ ). The assembly is shown in the diagram below (Fig

3). Voltages of the batteries were measured with a digital multimeter.



Figure 3: A diagram showing the assembly of a lithium ion battery

### III. Results and Discussion

#### A. Structure and Morphology

In order to determine that the desired structures of  $\text{TiO}_2$  were obtained, X-ray diffraction (XRD) was used to examine the crystalline structure of the samples. Data will be plotted on a graph of intensity against  $2\theta$  ( $2\theta$ ). The XRD patterns for the various phases of  $\text{TiO}_2$  are given the graphs below (Figure 4). With the  $310^\circ\text{C}$  and  $180^\circ\text{C}$  samples, diffraction peaks were obtained which were characteristic of the anatase structure of the  $\text{TiO}_2$  formed. No peaks were obtained for the XRD of the  $145^\circ\text{C}$  sample, showing that amorphous nature of the  $\text{TiO}_2$ . Further analysis of the cell parameters (Table 2) agreed with the theoretical data shown above.(Table1)

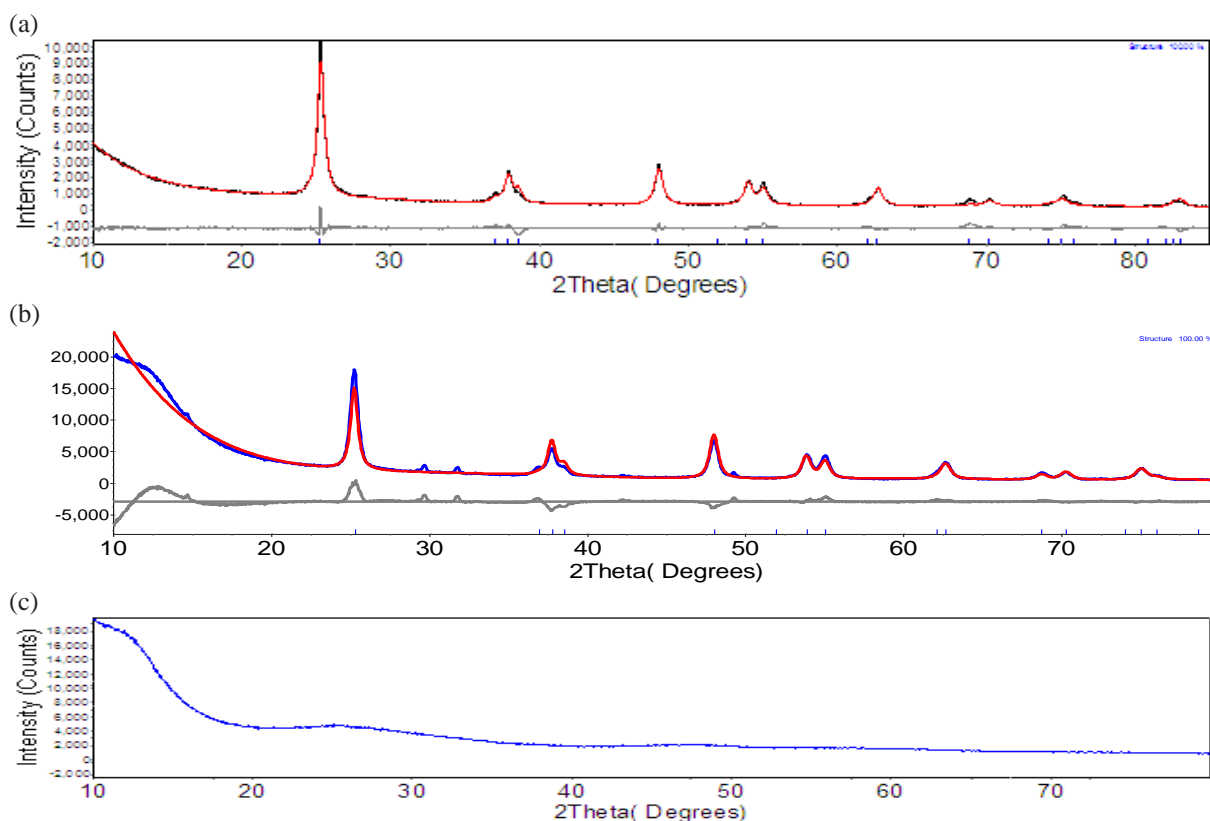


Figure 4: XRD patterns of  $\text{TiO}_2$  prepared at various temperatures, (a)  $310^\circ\text{C}$  (b)  $180^\circ\text{C}$  (c)  $145^\circ\text{C}$

Table 2: Experimental lattice parameters of the crystalline  $\text{TiO}_2$

Synthesis Temperature for $\text{TiO}_2$ / $^\circ\text{C}$	Experimental Lattice Parameters / $\text{\AA}$	
	a	c
310	3.7932648	9.5013898
180	3.7855469	9.5172376

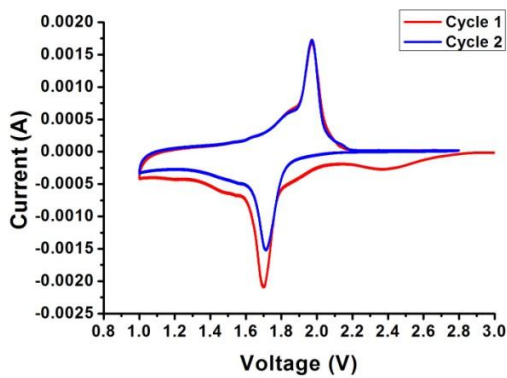
## B. Electrochemical Characteristics

### Cyclic Voltammetry (CV)

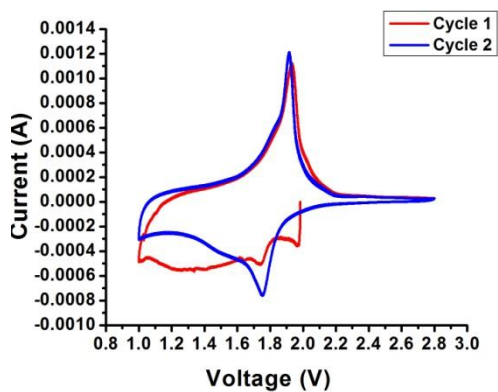
Cyclic Voltammetry (CV) was conducted on the cells using Mac-pile II (Bio-logic, France) at a scan rate of  $0.058 \text{ mV s}^{-1}$  and with the voltage ranging from 1.0 to 2.8 V vs Li. The graphs for the selected cycles for the cells are given below. Sharp peaks were obtained when the  $\text{TiO}_2$  sample was prepared at  $310^\circ\text{C}$  and  $180^\circ\text{C}$ . However, there were no peaks observed for the  $\text{TiO}_2$   $145^\circ\text{C}$  sample. During the anodic scan of  $\text{TiO}_2$  -  $310^\circ\text{C}$  a sharp peak was observed at 2.0V while during the cathodic scan, a sharp peak was observed at 1.7V. (Fig 4a) The cathodic and anodic peaks at 1.7 and 2.0V correspond to reduction and oxidation of  $\text{Ti}^{4+}$  to  $\text{Ti}^{3+}$  and  $\text{Ti}^{3+}$  to  $\text{Ti}^{4+}$ . The voltage hysteresis, calculated via the difference in potential for the cathodic and anodic peak in this sample was 0.3V.

For the  $\text{TiO}_2$  -  $180^\circ\text{C}$  sample, a sharp peak was observed at 1.9V during the anodic scan. For the cathodic scan, the peak was less sharp for cycle 1 with a range of 1.7V to 1.9V. (Fig 4b) Voltage hysteresis was calculated to be approximately 0V to 0.2V. For the  $310^\circ\text{C}$  and  $180^\circ\text{C}$  samples, the anatase nature of the  $\text{TiO}_2$  allowed for rapid diffusion of electrons in and out of the lattice. When this happens, Titanium ion is reduced and oxidised at very sharp voltages shown in the graphs. For the  $145^\circ\text{C}$  sample, the amorphous nature of the  $\text{TiO}_2$  sample indicates that electrons are unable to reduce and oxidise the titanium ions properly due to the random arrangements of the atoms and hence a range of oxidation and reduction voltages is shown.

(a)



(b)



(c)

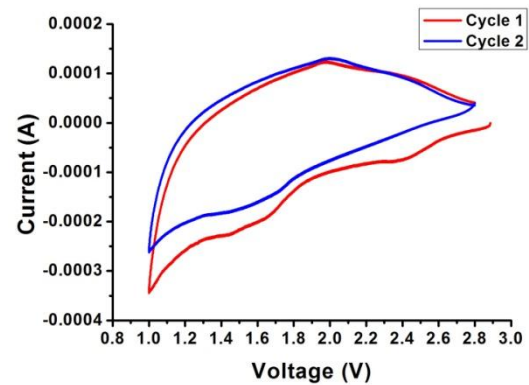


Figure 4: Cyclic voltammograms of sample at (a)  $310^\circ\text{C}$  (b)  $180^\circ\text{C}$  (c)  $145^\circ\text{C}$ , Scan rate:  $0.058 \text{ mV/sec}$ .

### C. Galvanostatic Cycling (GC)

Galvanostatic Cycling (GC) was conducted on the samples using a multi-channel battery tester (Model SCN, Bitrode, USA). The galvanostatic cycling was run from 1.0 to 3.0 V vs Li, and at a current rate of  $33 \text{ mA g}^{-1}$ . The voltage-capacity graphs (Fig 5) and the capacity-cycle number graphs (Fig 6) are given below. These plateaux correspond to the interaction of the Li ions with the  $\text{TiO}_2$  crystal structure. During charge and discharge of the  $\text{TiO}_2$ -  $145^\circ\text{C}$  sample, the amorphous phases showed broad peaks and no distinct plateaux (Fig 5c). The calculated capacity fading at  $-2.49\%$  (Fig 6c) was anomalous, and could be due to the structure of the  $\text{TiO}_2$ . Results obtained for this sample proved that amorphous structure of  $\text{TiO}_2$  were of limited use due to its weak electrochemistry.

Crystalline materials showed sharp peaks (Fig 5a). This is due to the distinct structures of  $\text{TiO}_2$  formed during the synthesis stage, resulting in good profiles for the charge-discharge cycles. During the charging process, a plateau at 1.8V vs. Li was observed, while a plateau at 1.7 V vs. Li was observed during the discharging process for the  $310^\circ\text{C}$  sample. (Fig 5a). It was noted that the capacity fading for the  $310^\circ\text{C}$  sample was low, at only 12.5%. Due to its low capacity fading,  $\text{TiO}_2$  –  $310^\circ\text{C}$  has potential applicability in electronics which require a low capacity fading over a large charge-discharge cycle. [Gordon-Bloomfield, 2015]

For the  $180^\circ\text{C}$  sample the plateaux noted were less distinct than the  $310^\circ\text{C}$  sample. A plateau was noted at 1.9 V vs. Li during the charging process while a plateau was noted at 1.8 V vs. Li during the discharging process. Capacity fading was particularly high at 68.9%.

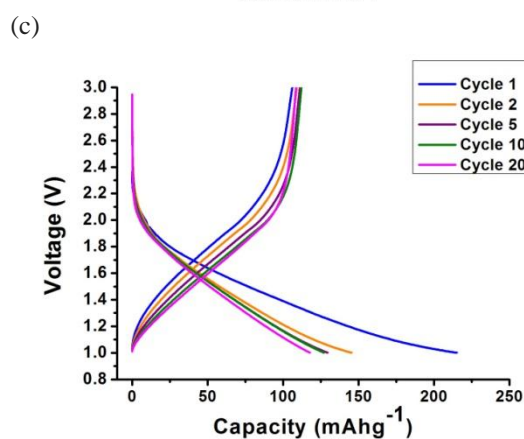
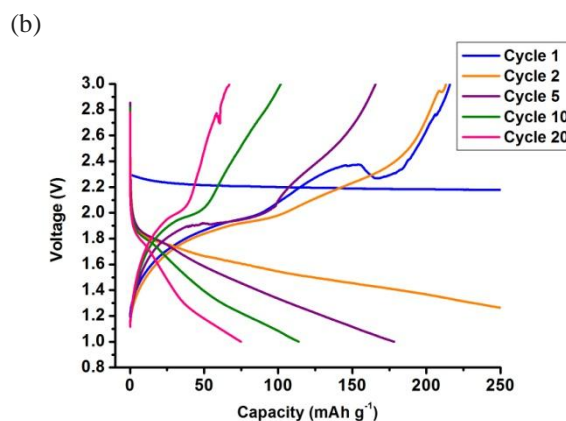
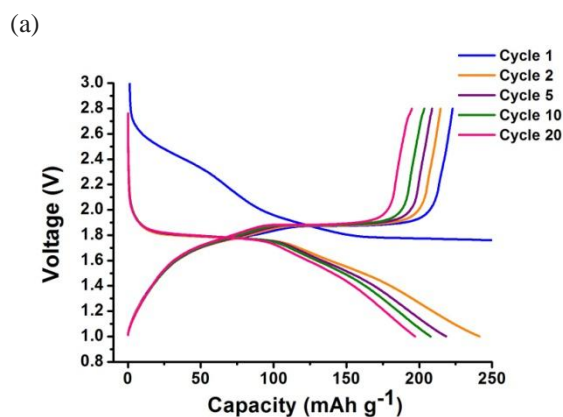
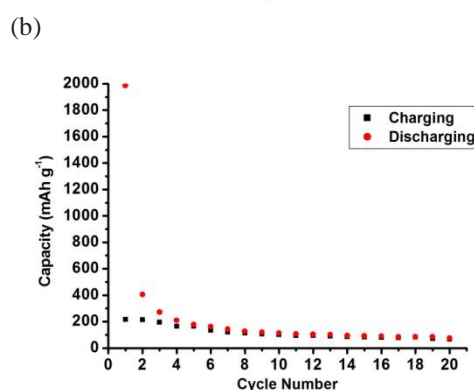
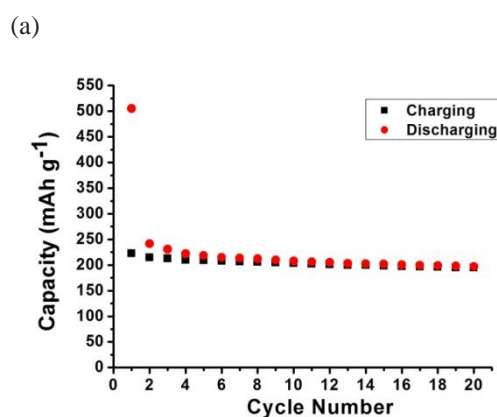


Figure 5: Voltage-capacity graphs for sample with temperature at (a)  $310^\circ\text{C}$  (b)  $180^\circ\text{C}$  (c)  $145^\circ\text{C}$



(c)

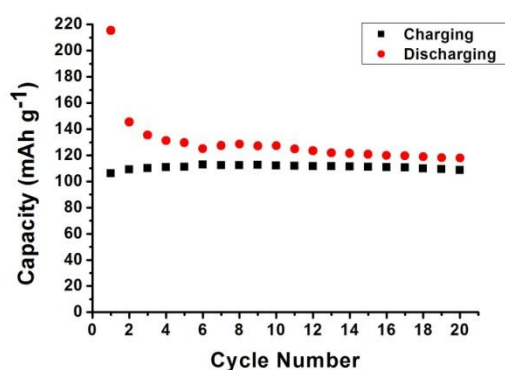


Figure 6: Capacity-cycle number graphs for the sample at (a) 310 °C (b) 180 °C (c) 145 °C

Table 3: Summary of the capacity changes in the cell samples

Preparation Temperature / °C	Initial Charge/Discharge Capacity / mAh g <sup>-1</sup>	Capacity at 20 <sup>th</sup> Cycle / mAh g <sup>-1</sup>	Capacity Fading / %
145	106.07	108.64	-2.49
180	215.94	67.12	68.9
310	222.86	194.98	12.5

#### IV. Conclusion

Crystalline nanoparticles of TiO<sub>2</sub> have been synthesised via the Molten Salt method at different synthesis temperatures. It is evident that synthesis temperature has an effect on the electrical properties of the battery. For TiO<sub>2</sub> - 145 °C, it shows an amorphous phase, as shown through XRD analysis. At different temperatures, the electrochemical properties of the cells are different. At higher temperatures such as 310 °C, the anatase structure dominates, allowing for high surface area for TiO<sub>2</sub> / Li<sup>+</sup> intercalation interactions. It should also be noted that the capacity fading of the cell increases with the synthesis temperature used for the electrodes, where TiO<sub>2</sub> - 145 °C has the lowest capacity fading of -2.49 %, while 180 °C has the highest capacity fading of 68.9%. To expand upon this project, further experiments could be conducted on a wider range of temperatures such as those within the range of 200 °C to 300 °C and the range between 400 °C to 800 °C. We could also investigate the electrochemical properties of TiO<sub>2</sub> synthesised through other methods such as the Sol Gel method, and the hydrothermal method, which may alter the electrochemical characteristics of the LIBs.

#### References

- Ortiz, G., Hanzu, I., Djenizian, T., Lavela, P., Tirado, J., & Knauth, P. (2009). Alternative Li-Ion Battery Electrode Based on Self-Organized Titania Nanotubes. *Chemistry of Materials Chem. Mater.*, 63-67.
- Khataee, A., & Mansoori, G. (2012). Properties of Titanium Dioxide and its Nanoparticles. In *Nanostructured titanium dioxide materials properties, preparation and applications* (p. 5, 20). Singapore: World Scientific.
- Aleman, L., Bañares, M., Pardo, E., Martín-Jiménez, F., & Blasco, J. (n.d.). Morphological and Structural Characterization of a Titanium Dioxide System. *Materials Characterization*, 271-275.
- Chen, X., & Mao, S. (n.d.). Titanium Dioxide Nanomaterials: Synthesis, Properties, Modifications, and Applications. *Chemical Reviews Chem. Rev.*, 2892-2901. doi:10.1021/cr0500535
- Johnson, B., & White, R. (n.d.). Characterization of commercially available lithium-ion batteries. *Journal of Power Sources*, 70(1), 48-54. doi:10.1016/S0378-7753(97)02659-1
- Reddy, M., Kishore, M., Pralong, V., Caignaert, V., Varadaraju, U., & Raveau, B. (n.d.). Room temperature synthesis and Li insertion into nanocrystalline rutile TiO<sub>2</sub>. *Electrochemistry Communications*, 8(8), 1299-1303. doi:10.1016/j.elecom.2006.05.021
- Arora, P. (n.d.). Capacity Fade Mechanisms and Side Reactions in Lithium-Ion Batteries. *Journal of The Electrochemical Society J. Electrochem. Soc.*, 145(10), 3647-3647. doi:10.1149/1.1838857
- Doughty, D., & Roth, E. (2012). A General Discussion of Li Ion Battery Safety. *Interface*, 37-44.
- Reddy, M., Adams, S., Aloysius, C., & Chowdari, B. (n.d.). Effect of molten salt synthesis temperature on TiO<sub>2</sub> and Li-cycling properties.
- Despite Capacity Loss, Today's Entry-Level Electric Cars Can Meet 85% of Driving Needs, Says DoE Scientists. (2015, March 31). Retrieved January 5, 2016, from <https://transportevolved.com/2015/03/31/despite-capacity-loss-todays-entry-level-electric-cars-can-meet-85-of-driving-needs-says-doe-scientists/>